

Reversible Multicomponent Self-Assembly Mediated By Bismuth Ions

Amber M. Johnson, Michael C. Young and Richard J. Hooley.*

Department of Chemistry, University of California, Riverside, CA 92521.

richard.hooley@ucr.edu

Electronic Supplementary Information

1. Mass Spectral Data

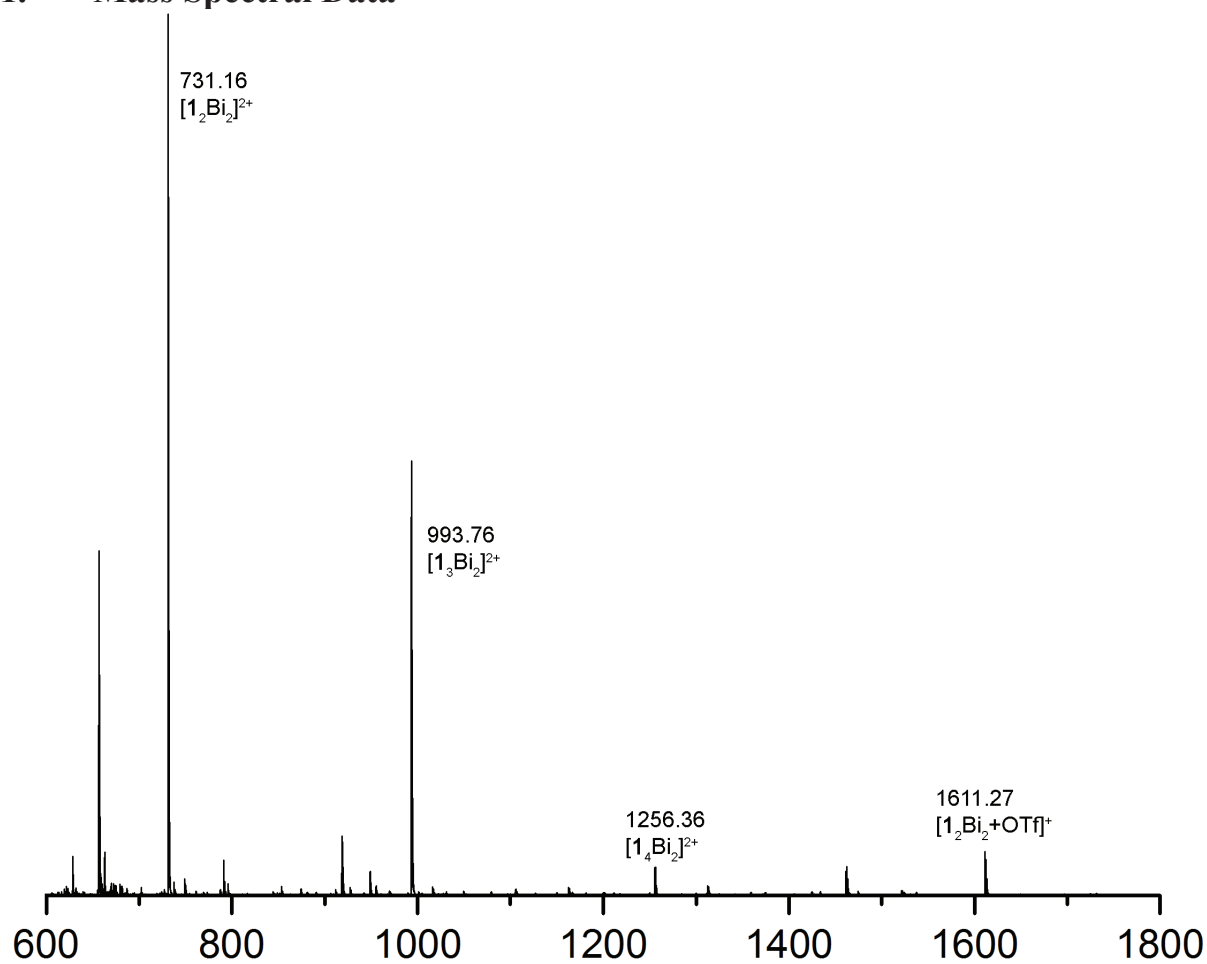


Figure S-1. Full ESI-MS spectra (MeCN) of **1** + $\text{Bi}(\text{OTf})_3$ indicating formation of the M_2L_2 , M_2L_3 , and M_2L_4 complexes.

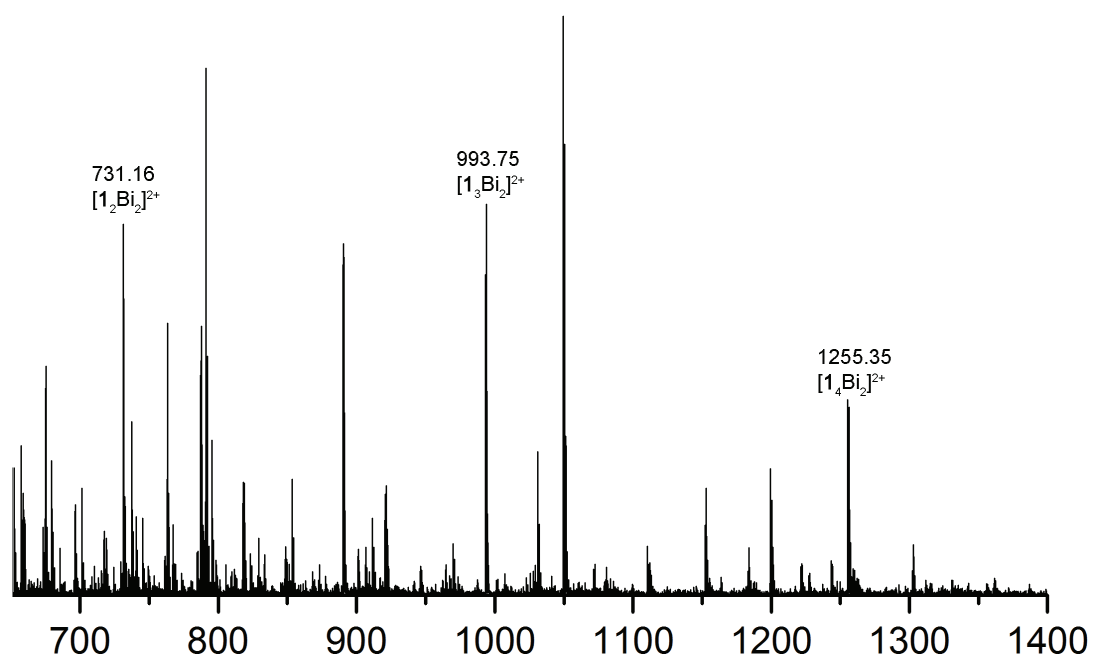


Figure S-2. ESI-MS spectra (MeCN) of **1** + 0.5 eq $\text{Bi}(\text{OTf})_3$ showing enhancement of the M_2L_4 complex.

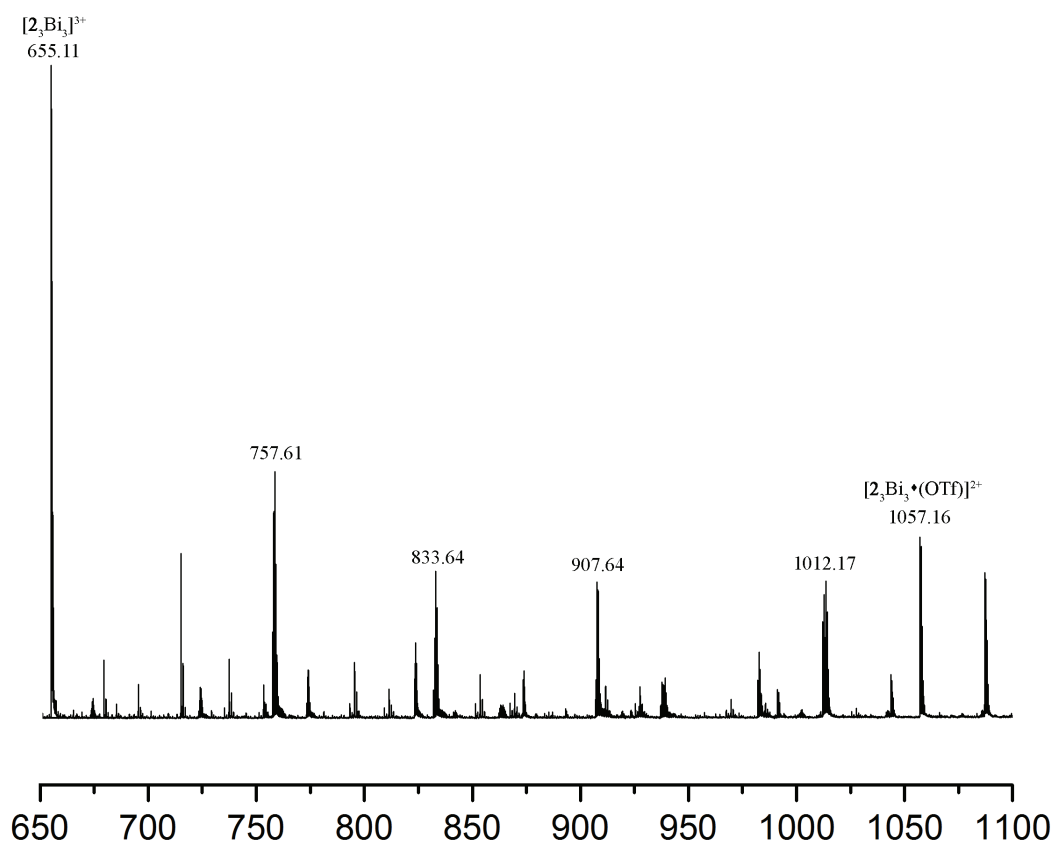


Figure S-3. ESI-MS spectra (MeCN) of $2_3\text{Bi}_3 \cdot 9\text{OTf}$ and undefined aggregates.

2. NMR Spectra of Synthesized Compounds

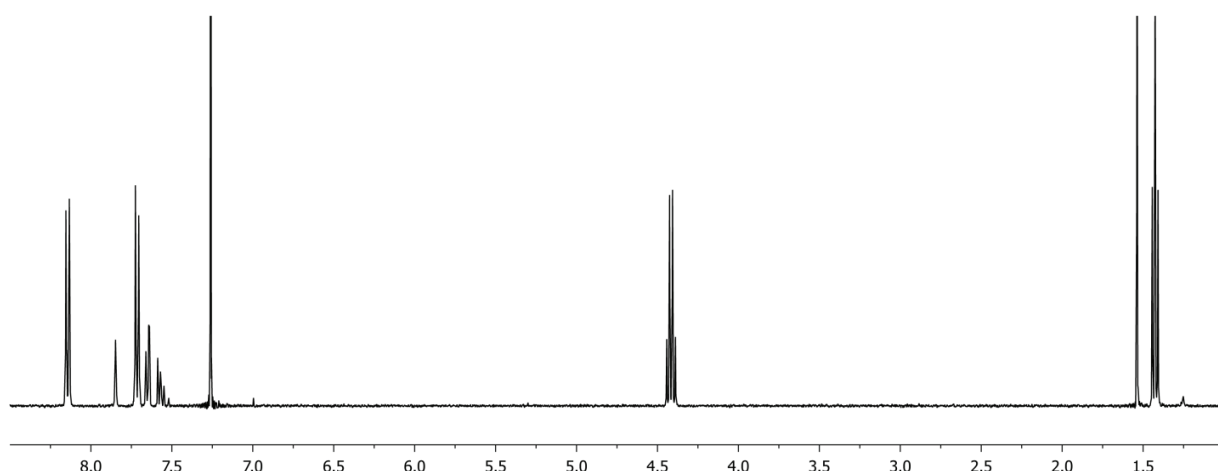


Figure S-4. ¹H NMR spectrum of diethyl 1,1':3',1''-terphenyl-4,4''-dicarboxylate (CDCl₃, 400 MHz, 298K)

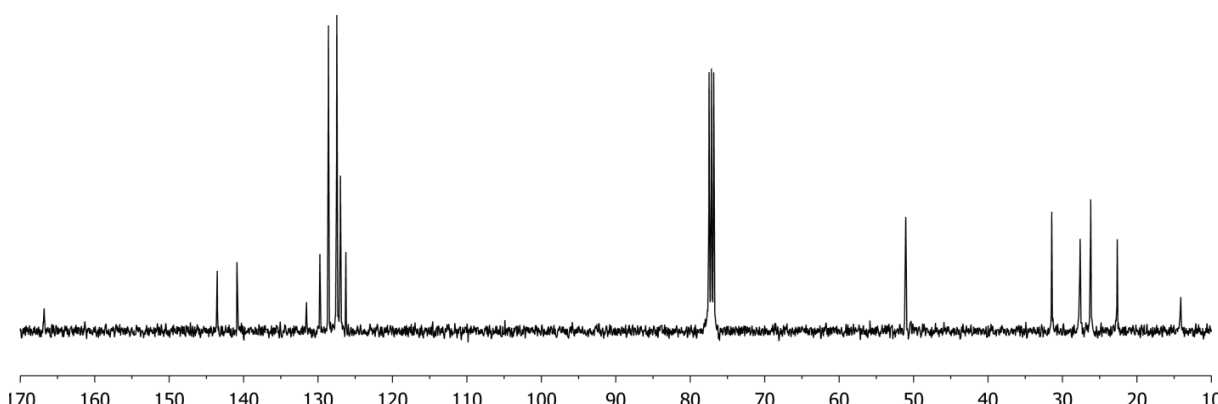


Figure S-5. ¹³C NMR spectrum of diethyl 1,1':3',1''-terphenyl-4,4''-dicarboxylate (CDCl₃, 100 MHz, 298K)

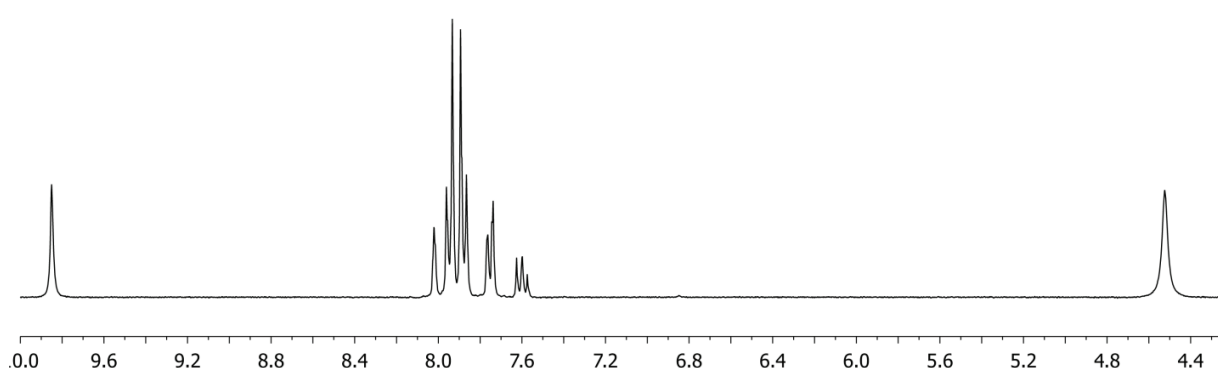


Figure S-6. ¹H NMR spectrum of hydrazide **3** (DMSO-*d*₆, 400 MHz, 298K)

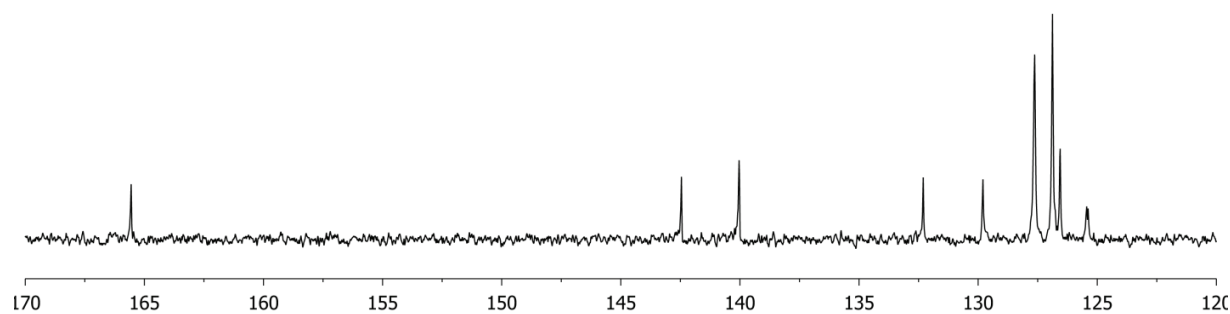


Figure S-7. ^{13}C NMR spectrum of hydrazide **3** (DMSO- d_6 , 100 MHz, 298K)

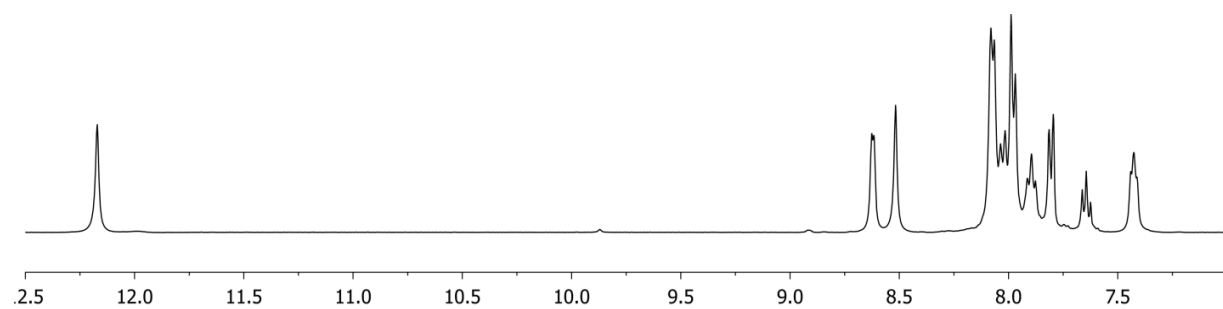


Figure S-8. ^1H NMR spectrum of hydrazone ligand **1** (DMSO- d_6 , 400 MHz, 298K)

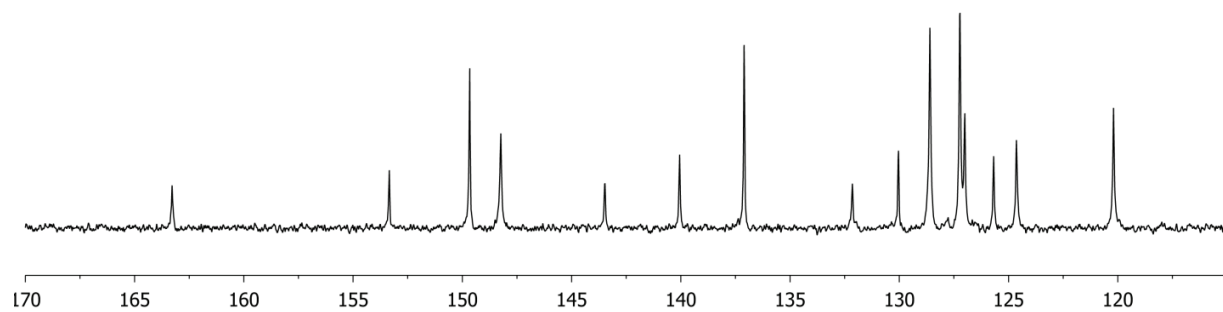


Figure S-9. ^{13}C NMR spectrum of hydrazone ligand **1** (DMSO- d_6 , 100 MHz, 298K)

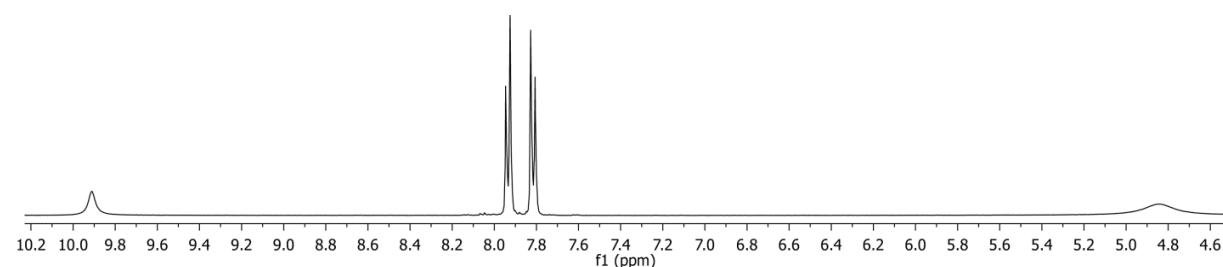


Figure S-10. ^1H NMR spectrum of hydrazide **4** (DMSO- d_6 , 400 MHz, 298K)

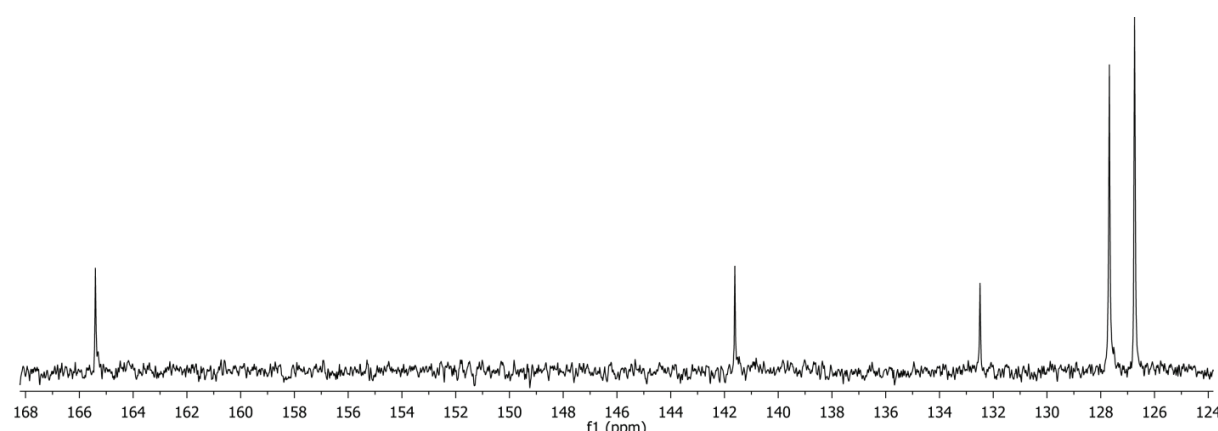


Figure S-11. ¹³C NMR spectrum of hydrazide 4 (DMSO-*d*₆, 100 MHz, 298K)

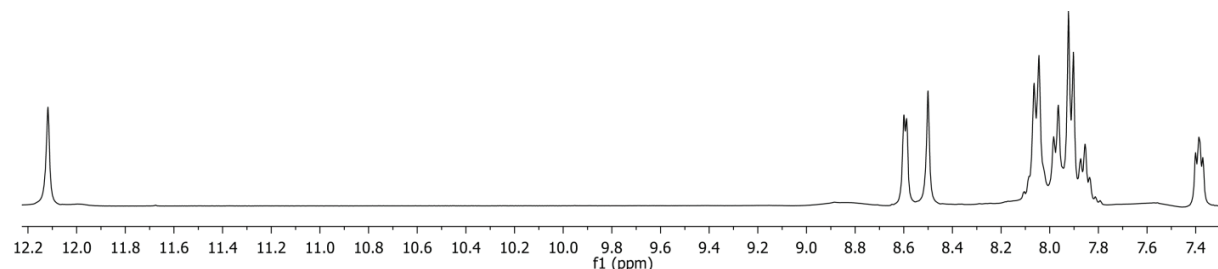


Figure S-12. ¹H NMR spectrum of hydrazone ligand 2 (DMSO-*d*₆, 400 MHz, 298K)

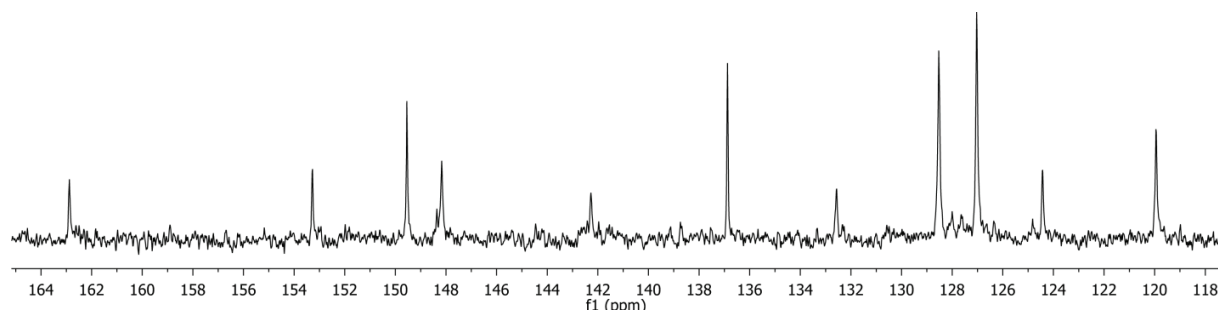


Figure S-13. ¹³C NMR spectrum of hydrazone ligand 2 (DMSO-*d*₆, 100 MHz, 298K)

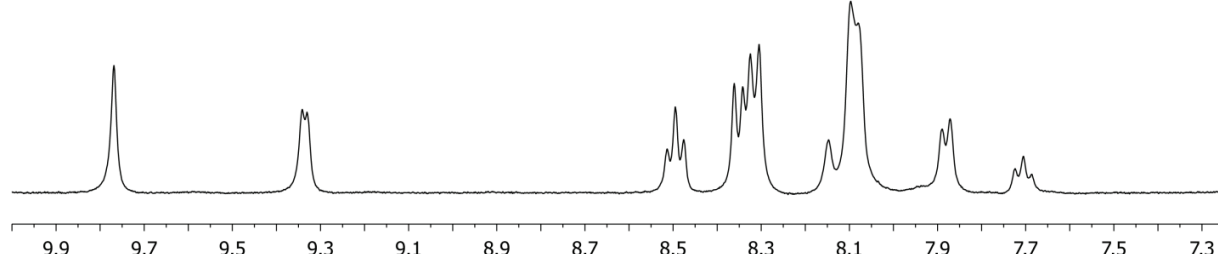


Figure S-14. ¹H NMR spectrum of self-assembled complex **1₂Bi₂·6(OTf)** (CD₃CN, 400 MHz, 298K)

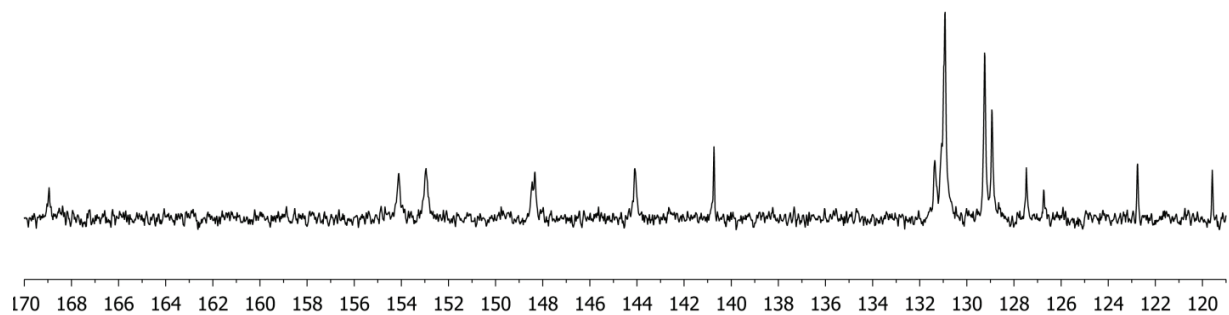


Figure S-15. ¹³C NMR spectrum of self-assembled complex **1₂Bi₂·6(OTf)** (CD₃CN, 100 MHz, 298K)

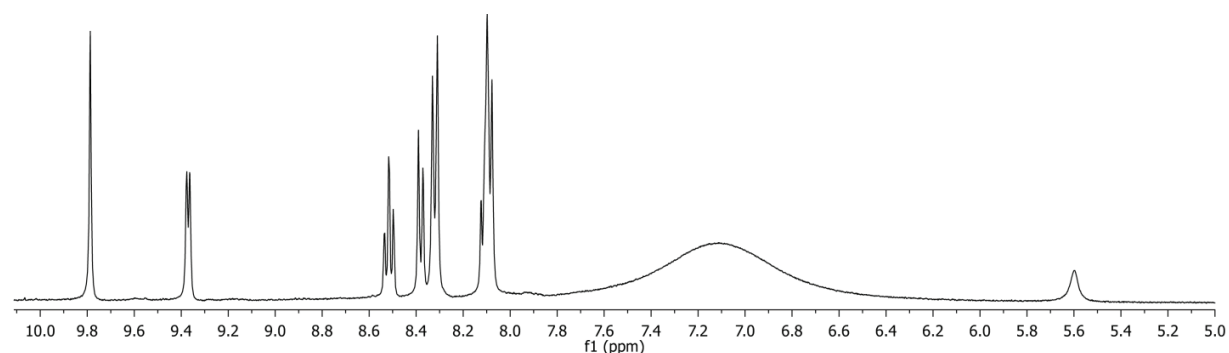


Figure S-16. ¹H NMR spectrum of self-assembled complex **2₃Bi₃·9(OTf)** (CD₃CN, 400 MHz, 298K)

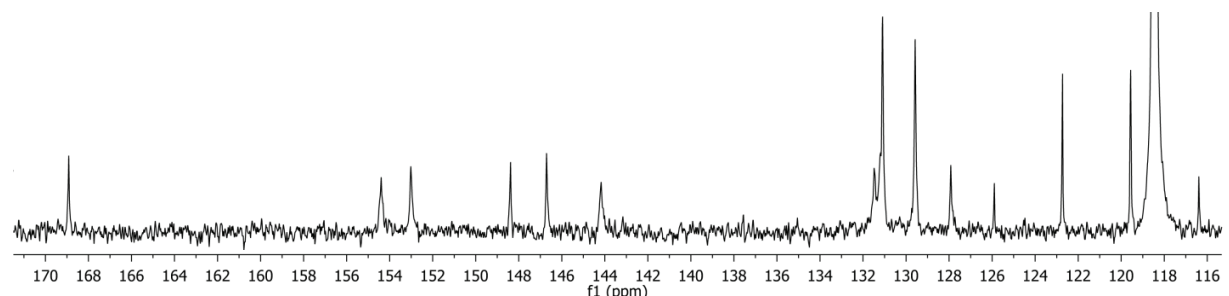


Figure S-17. ¹³C NMR spectrum of self-assembled complex **2₃Bi₃·9(OTf)** (CD₃CN, 100 MHz, 298K)

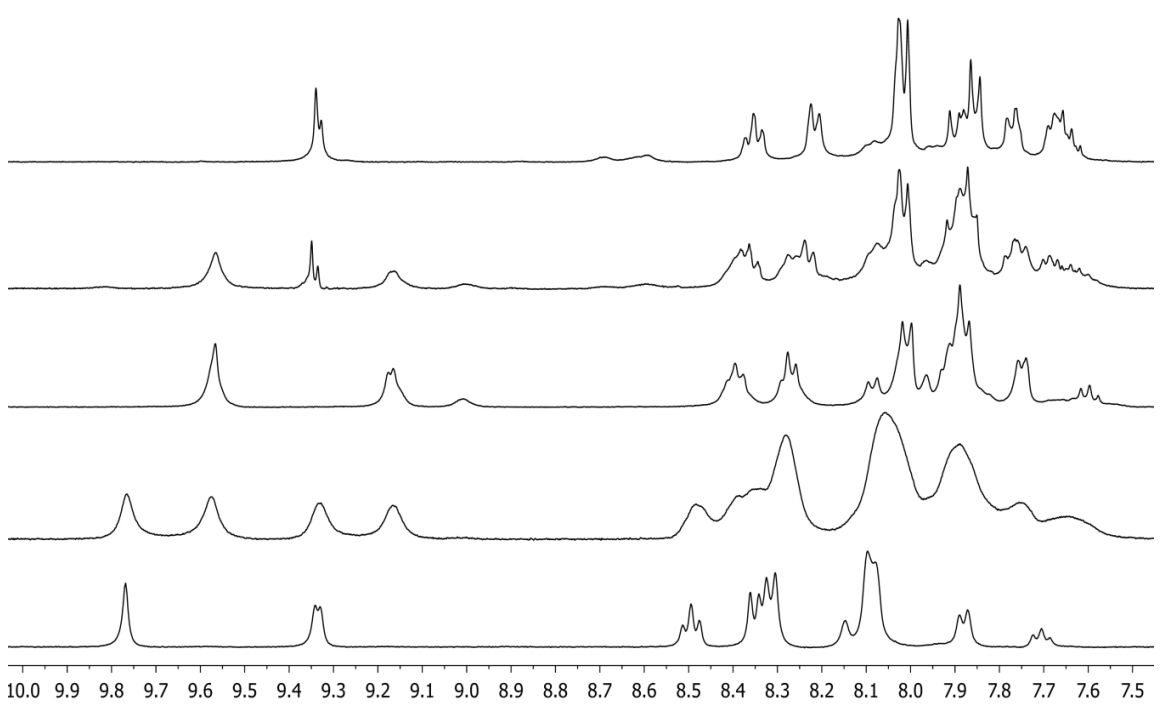


Figure S-18. ^1H NMR titration of $\text{Bi}(\text{OTf})_3$ into ligand **1**: (a) 0.5 eq; (b) 0.67 eq; (c) 1 eq; (d) 2 eq; (e) 3 eq; (CD_3CN , 400 MHz, 298 K)

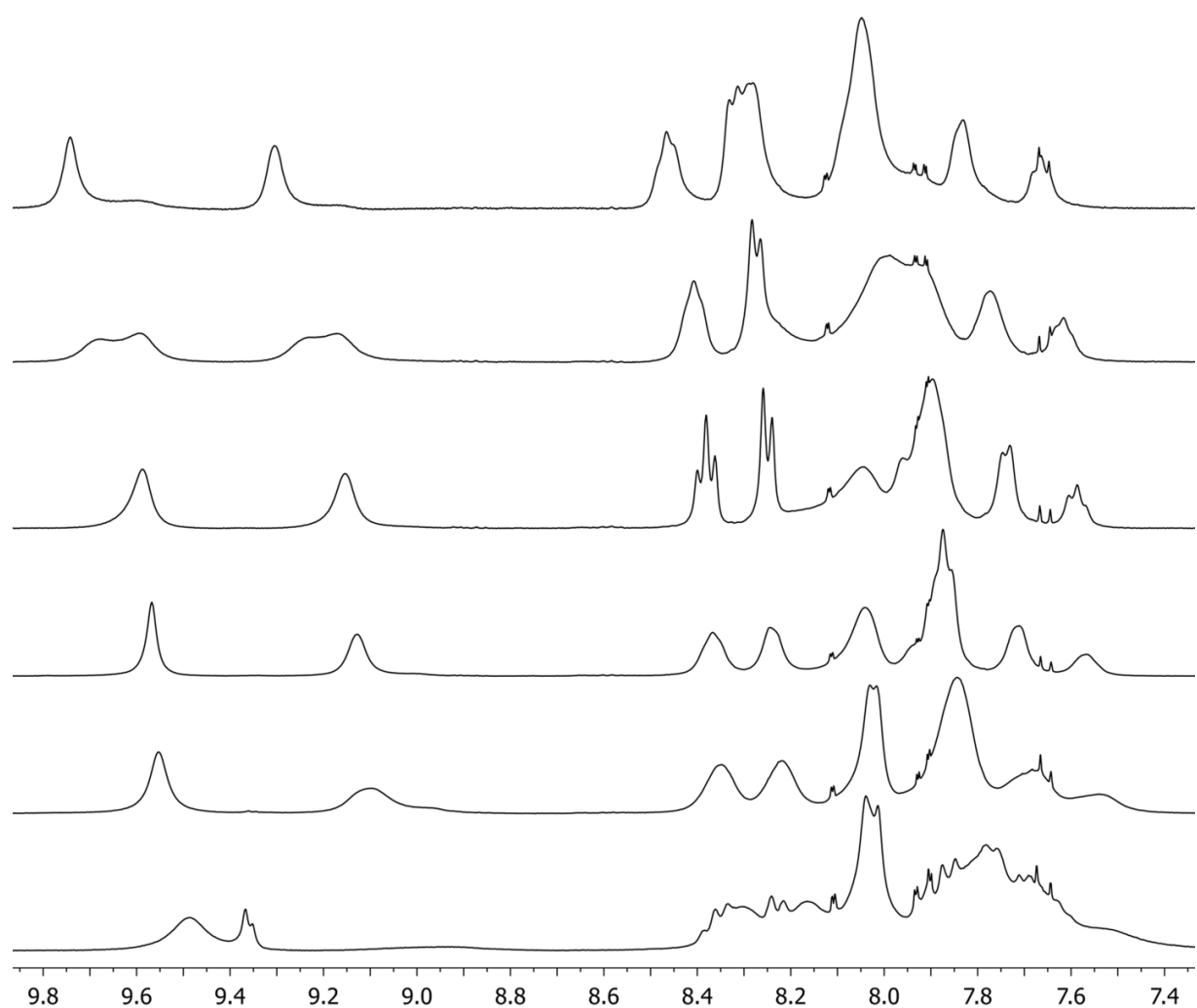


Figure S-19. ^1H NMR titration of ligand **1** into $\mathbf{1}_2 \cdot \text{Bi}_2$: (a) $\mathbf{1}_2 \cdot \text{Bi}_2$; (b) 1.0 eq; (c) 1.8 eq; (d) 2.9 eq; (e) 4.2 eq; (f); 6.0 eq; (CD_3CN , 400 MHz, 298 K)

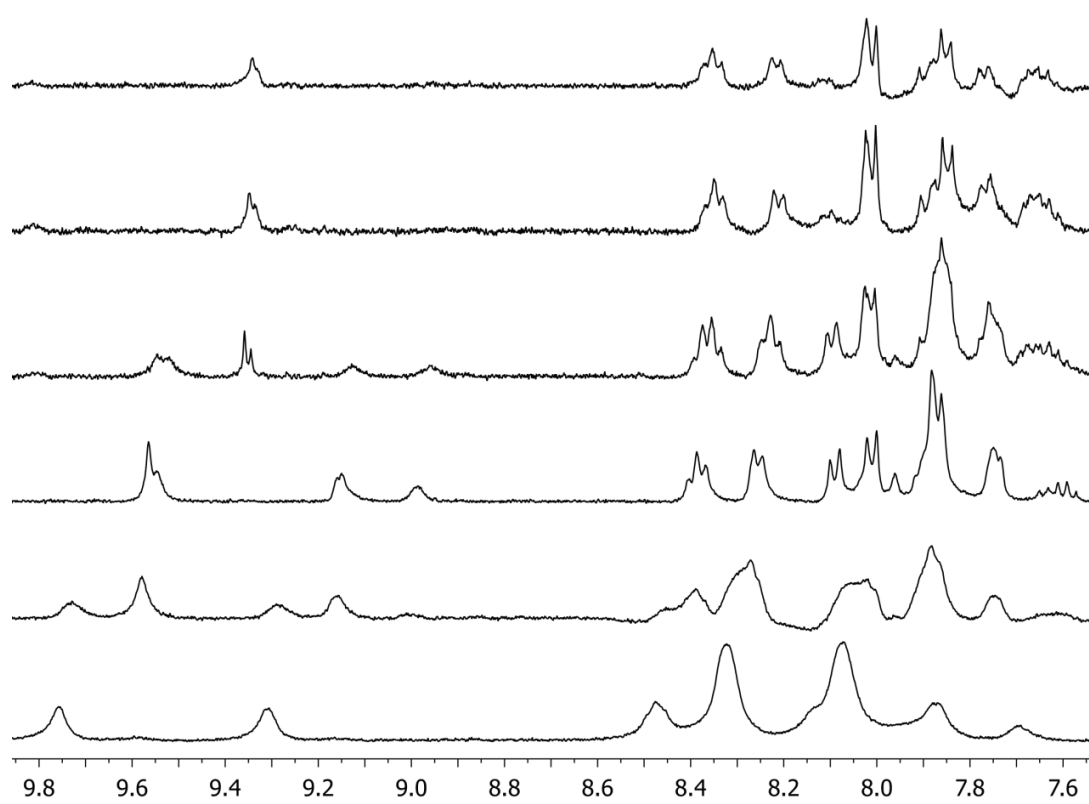


Figure S-20. ¹H NMR titration of Bi(OTf)₃ into ligand **1**·Na₂: (a) 0.5 eq; (b) 0.75 eq; (c) 1 eq; (d) 1.5 eq; (e) 3 eq; (f) 5 eq; (CD₃CN, 400 MHz, 298 K)

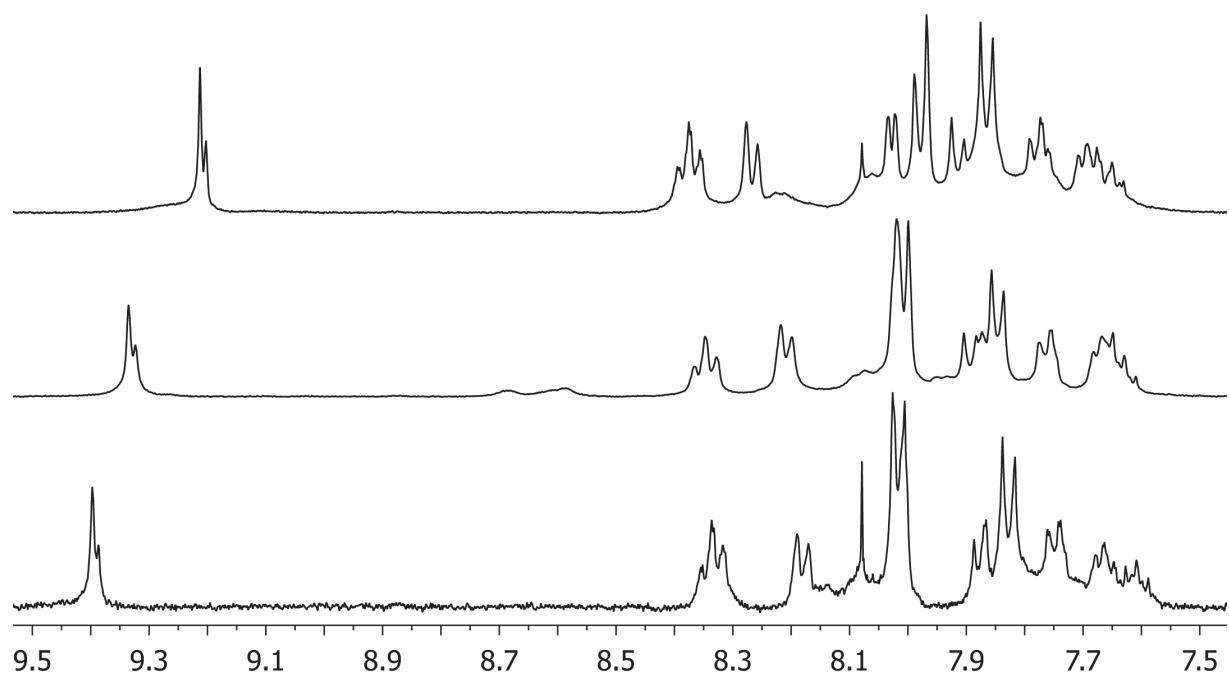


Figure S-21. Addition of sodium triflate to **1·Bi(BF₄)**: (a) **1·Bi(BF₄)**; (b) **1₄·Bi₂·OTf**; (c) **1·Bi(BF₄) + NaOTf** (CD₃CN, 400 MHz, 298 K).

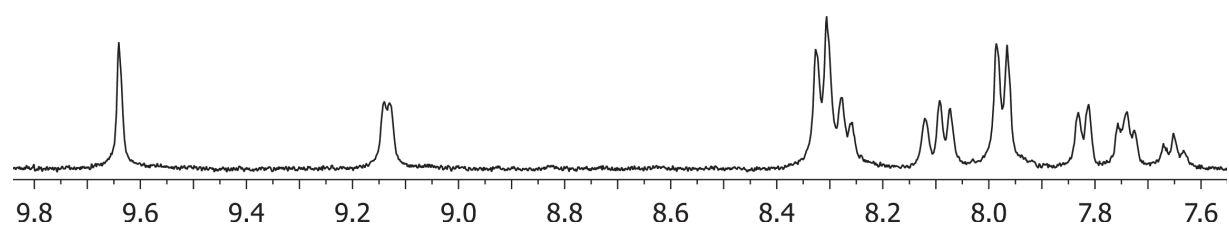


Figure S-22. ¹H NMR spectrum of complex **1·BiBr₃**. (DMSO-*d*₆, 400 MHz, 298 K)

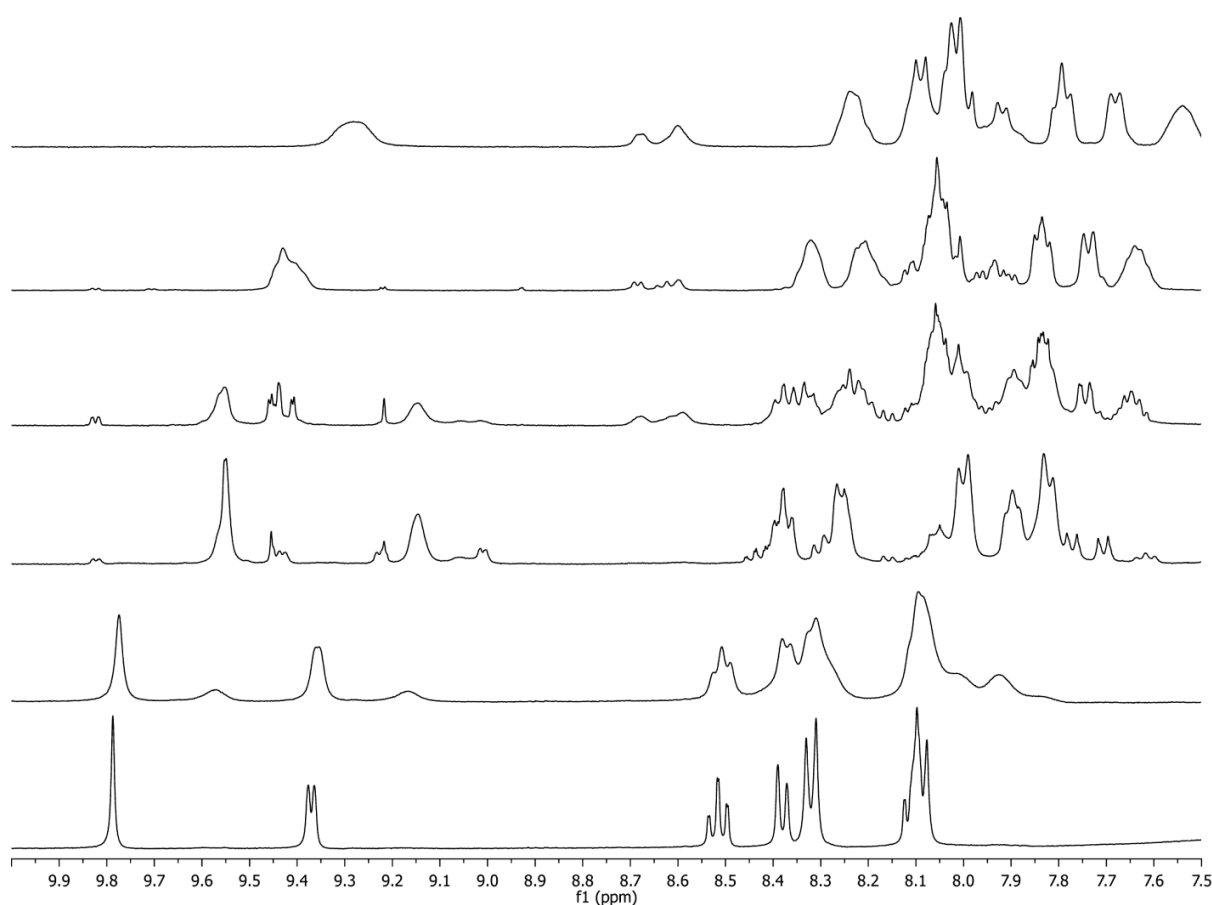


Figure S-23. ¹H NMR titration of Bi(OTf)₃ into ligand 2: (a) 0.33 eq; (b) 0.66 eq; (c) 1 eq; (d) 1.5 eq; (e) 2 eq; (f) 3 eq; (CD₃CN, 400 MHz, 298 K).

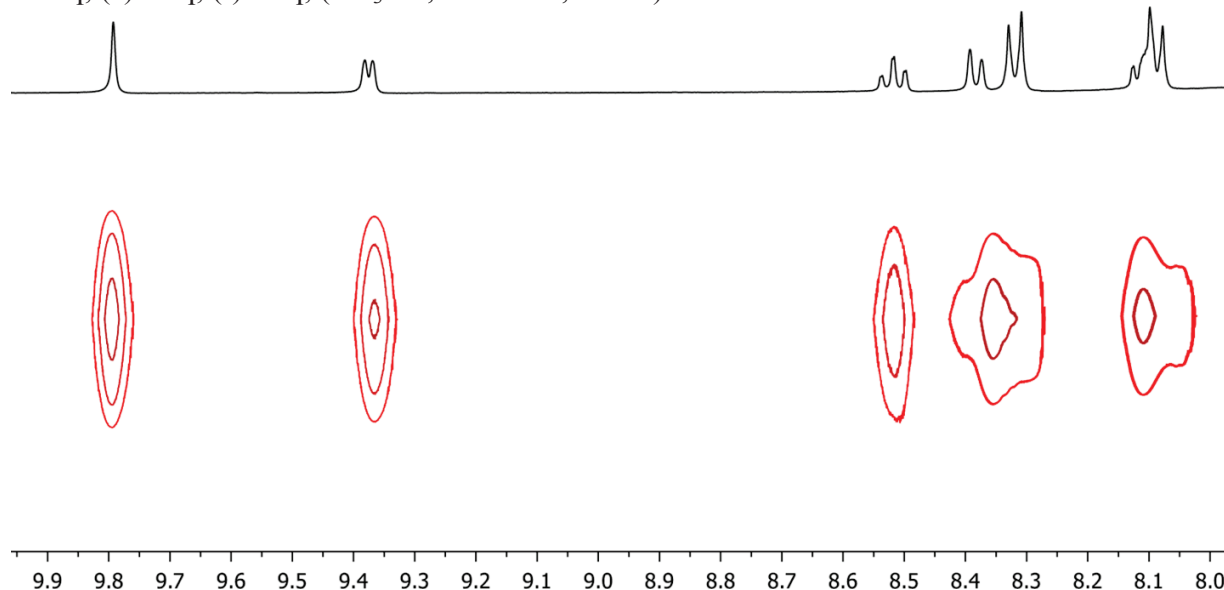
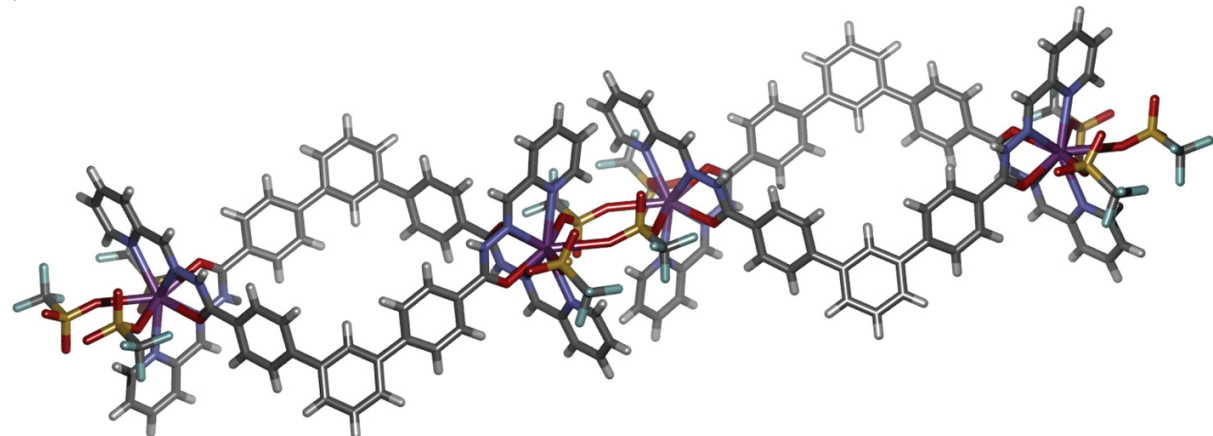


Figure S-24. DOSY-NMR of 2₃•Bi₃ (CD₃CN, 600 MHz, 298 K, Δ = 17 ms, δ = 7000 μs, Diffusion Coefficient = 4.88x10⁻¹⁰ m²/s).

3. X-Ray Structure Determination

a)



b)

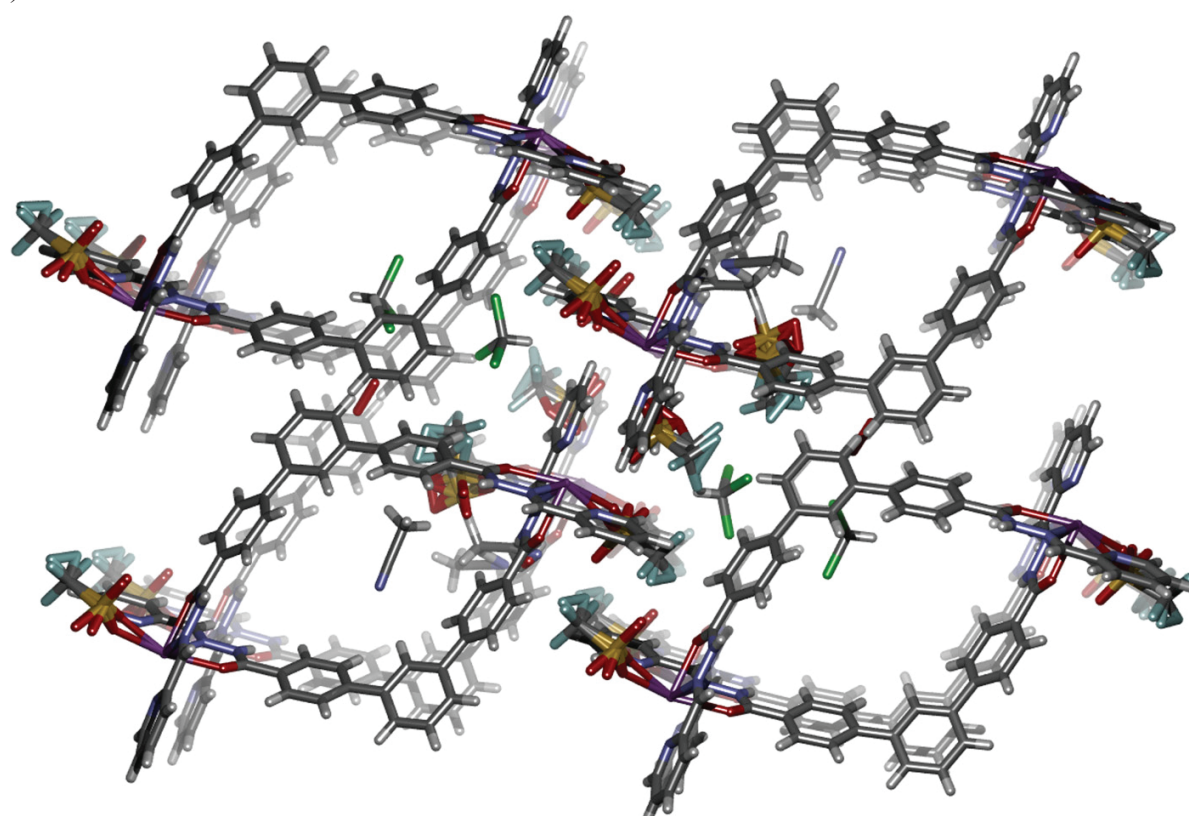


Figure S-25. a) Structure of the complex $\mathbf{1}_2 \cdot \text{Bi}_2 \cdot \text{OTf}_6$ as determined by X-ray diffraction analysis (counterions and solvent removed for clarity; b) Structure of the unit cell of complex $\mathbf{1}_2 \cdot \text{Bi}_2 \cdot \text{OTf}_6$, indicating disordered solvent molecules and triflate counterions.

A colorless fragment of a prism ($0.35 \times 0.17 \times 0.07 \text{ mm}^3$) was used for the single crystal X-ray diffraction study of **1₂•Bi₂•(OTf)₆** (CCDC submission #892045). The crystal was coated with paratone oil and mounted on to a cryo-loop glass fiber. X-ray intensity data were collected at 100(2) K on a Bruker APEX2¹ platform-CCD X-ray diffractometer system (fine focus Mo-radiation, $\lambda = 0.71073 \text{ \AA}$, 50KV/35mA power). The CCD detector was placed at a distance of 5.0000 cm from the crystal.

A total of 4800 frames were collected for a sphere of reflections (with scan width of 0.3° in ω or ϕ , starting ω and 2θ angles of -30° , and ϕ angles of $0^\circ, 90^\circ, 120^\circ, 180^\circ, 240^\circ$, and 270° for every 600 frames, and 1200 frames with ϕ -scan from $0-360^\circ$, 20 sec/frame exposure time). The frames were integrated using the Bruker SAINT software package² and using a narrow-frame integration algorithm. Based on a triclinic crystal system, the integrated frames yielded a total of 68323 reflections at a maximum 2θ angle of 54.96° (0.77 Å resolution), of which 13040 were independent reflections ($R_{\text{int}} = 0.0256$, $R_{\text{sig}} = 0.0194$, redundancy = 5.2, completeness = 99.8%) and 12130 (93.0%) reflections were greater than $2\sigma(I)$. The unit cell parameters were, **a** = $10.5697(3) \text{ \AA}$, **b** = $13.7043(4) \text{ \AA}$, **c** = $20.0249(6) \text{ \AA}$, $\alpha = 98.057(1)$, $\beta = 92.112(1)^\circ$, $\gamma = 96.452(1)$ V = $2849.71(14) \text{ \AA}^3$, Z = 2, calculated density $D_c = 1.622 \text{ g/cm}^3$. Absorption corrections were applied (absorption coefficient $\mu = 3.433 \text{ mm}^{-1}$; max/min transmission = 0.8001/0.3770) to the raw intensity data using the SADABS program.³

The Bruker SHELXTL software package⁴ was used for phase determination and structure refinement. The distribution of intensities and no systematic absent reflections indicated two possible space groups, P-1 and P1. The space group P-1 (#2) was later determined to be correct. Direct methods of phase determination followed by two Fourier cycles of refinement led to an electron density map from which most of the non-hydrogen atoms were identified in the asymmetry unit of the unit cell. With subsequent isotropic refinement, all of the non-hydrogen atoms were identified. There were one ligand of C₃₂H₂₄N₆O₂, one Bi-cation, three disordered SO₃CF₃ anions (site occupancy ratios are 80%/20%, 81%/19%, 75%/25%), one disordered CHCl₃ (site occupancy ratio is 58%/42%), one disordered CH₃CN (site occupancy ratio is 73%/27%), one partially occupied CH₃CN (80% occupied), and two partially occupied H₂O (66% and 39% occupied) present in the asymmetry unit of the unit cell. The 39% occupied water

molecule near the inversion centered was modeled without its hydrogen atoms. One of the two H-atoms of the 66% occupied water didn't have an H-atom acceptor within the rigid model distance as the H-acceptor. All the alerts level B, C and G warning are either because of disordered and partially occupied solvents (water, acetonitrile and chloroform) or the disordered SO_3CF_3 anions. All possible hydrogen bonding distances and angles are given in Table 7. The DFIX, SADI, SIMU, DELU, and EADP, restraints were to stabilize the final refinement of the atomic positions. Although the distribution of intensities ($E^2 - 1 = 0.705$) indicated a possible racemic twin P1 chiral space group, the refinement using the racemic twin P1 space group was highly unstable for most of the solvent molecules giving rise to non-definite positive thermal parameters. The final structure model was refined using the P-1 space group.

Atomic coordinates, isotropic and anisotropic displacement parameters of all the non-hydrogen atoms were refined by means of a full matrix least-squares procedure on F^2 . The H-atoms were included in the refinement in calculated positions riding on the atoms to which they were attached, except the two NH-group hydrogen atoms were refined unrestrained. The refinement converged at $R1 = 0.0293$, $wR2 = 0.0774$, with intensity, $I > 2\sigma(I)$. The largest peak/hole in the final difference map was $1.675/-0.680 \text{ e}/\text{\AA}^3$. The high electron density peak/hole ratio (2.46) near the Bi-atom was probably due to absorption correction error.

Table S-1. Crystal data and structure refinement for **1₂•Bi₂•(OTf)₆**.

Empirical formula	[C ₃₂ H ₂₄ N ₆ O ₂] ₂ [Bi] ₂ [SO ₃ CF ₃] ₆
Formula weight	1391.94
Temperature	100(2) K
Wavelength	0.71073 Å
Crystal system	Triclinic
Space group	P-1 (#2)
Unit cell dimensions	$a = 10.5697(3)$ Å $\alpha = 98.057(1)^\circ$. $b = 13.7043(4)$ Å $\beta = 92.112(1)^\circ$. $c = 20.0249(6)$ Å $\gamma = 96.452(1)^\circ$.
Volume	2849.71(14) Å ³
Z	2
Density (calculated)	1.622 Mg/m ³
Absorption coefficient	3.433 mm ⁻¹
$F(000)$	1366
Crystal size	0.35 x 0.17 x 0.07 mm ³
Theta range for data collection	1.51 to 27.48°.
Index ranges	-13≤ h ≤13, -17≤ k ≤17, -25≤ l ≤25
Reflections collected	68323
Independent reflections	13040 [R _{int} = 0.0256]
Completeness to $\theta = 27.48^\circ$	99.8 %
Absorption correction	Semi-empirical from equivalents
Max. and min. transmission	0.8001 and 0.3770
Refinement method	Full-matrix least-squares on F^2
Data / restraints / parameters	13040 / 849 / 981
Goodness-of-fit on I^2	1.077
Final R indices [I>2σ(I)]	R1 = 0.0293, wR2 = 0.0774
RI indices (all data)	R1 = 0.0328, wR2 = 0.0795
Largest diff. peak and hole	1.675 and -0.680 e.Å ⁻³

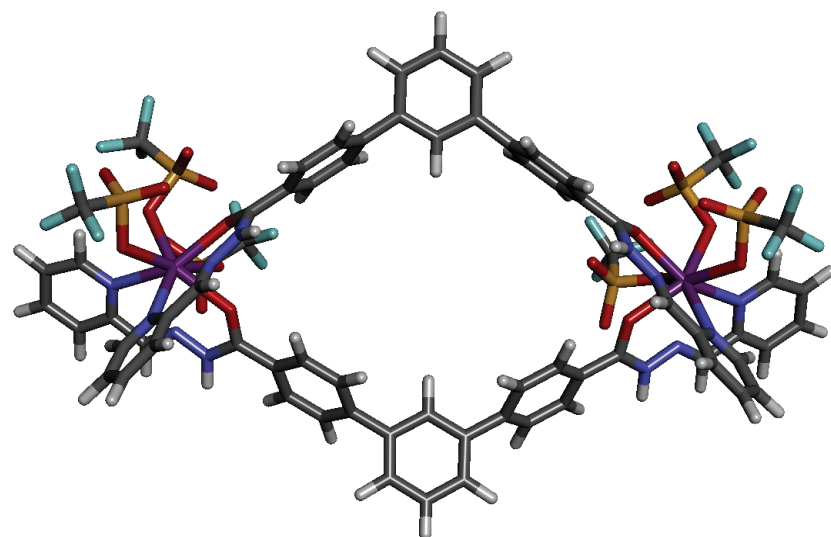


Figure S-26. a) Structure of the complex $\mathbf{1}_2 \bullet \text{Bi}_2 \bullet \text{OTf}_6$ as determined by molecular modeling (SPARTAN, AM1 forcefield).

References

- 1) *APEX 2*, version 2012.2-0, Bruker (2012), Bruker AXS Inc., Madison, Wisconsin, USA.
- 2) *SAINT*, version V8.18C, Bruker (2011), Bruker AXS Inc., Madison, Wisconsin, USA.
- 3) *SADABS*, version 2008/1, Bruker (2008), Bruker AXS Inc., Madison, Wisconsin, USA.
- 4) *SHELXTL*, version 2008/4, Bruker (2008), Bruker AXS Inc., Madison, Wisconsin, USA.